

## Depopulation of $^{180}\text{Ta}^m$ by Coulomb excitation and possible astrophysical consequences

C. Schlegel, P. von Neumann-Cosel, F. Neumeyer, A. Richter, and S. Strauch  
*Institut für Kernphysik, Technische Hochschule Darmstadt, D-64289 Darmstadt, Germany*

J. de Boer and C.H. Dasso\*  
*Sektion Physik, Universität München, D-85748 Garching, Germany*

R.J. Peterson  
*Nuclear Physics Laboratory, University of Colorado, Boulder, Colorado 80309*  
 (Received 11 May 1994)

The depopulation of  $^{180}\text{Ta}^m$  by Coulomb excitation was investigated in a thick-target experiment using beams of  $^{32}\text{S}$  and  $^{36}\text{S}$  with energies of 70–130 MeV on disks of natural tantalum. The resulting  $^{180}\text{Ta}$  ground-state population was measured by detecting its eight-hour decay. At the higher incident energies the observed  $^{180}\text{Ta}$  yield is dominated by sub-Coulomb neutron pickup transfer reactions on the  $10^4$  times more abundant  $^{181}\text{Ta}$ . At the lower incident energies the  $^{180}\text{Ta}$  ground-state yield is found to be compatible with Coulomb excitation of the isomer to an intermediate level with energies  $E_x < 1$  MeV and a reduced transition probability  $B(E2) \simeq 0.02\text{--}0.25$  Weisskopf units. Consequences for the astrophysical production mechanism of  $^{180}\text{Ta}$  are discussed.

PACS number(s): 23.20.-g, 25.20.Dc, 27.70.+q, 97.10.Cv

### I. INTRODUCTION

The element tantalum is the rarest in nature (0.02 with silicon normalized to  $10^6$ ). The odd-odd nucleus  $^{180}\text{Ta}$  is the rarest isotope with a relative abundance of only 0.012% and  $^{180}\text{Ta}^m$  is the only naturally occurring isomer. The survival of the excited state of  $^{180}\text{Ta}^m$  finds its explanation by the eight-times  $K$ -forbidden transition from the 73 keV  $J^\pi = 9^-$  isomer to the  $J^\pi = 1^+$  ground state. The large hindrance manifests itself in a lifetime  $T_{1/2} > 1.2 \times 10^{15}$  y [1] while the ground state (g.s.) decays with  $T_{1/2} = 8.1$  h.

The stellar production mechanism of the isomer remains an unresolved puzzle [2]. On the one hand  $^{180}\text{Ta}$  lies aside from the main path of the slow-neutron  $s$  process which proceeds through the chain of stable Hf isotopes; on the other hand it is shielded by the stable  $A = 180$  neighbors  $^{180}\text{Hf}$  and  $^{180}\text{W}$  from the  $\beta$ -decay paths following the rapid-neutron  $r$  process or the proton  $p$  process which account for the production of isotopes far away from the valley of stability. Several ideas have been put forward to explain the solar-system abundance through more complicated processes. Yokoi and Takahashi [3] proposed an  $s$ -process production by an excited-state  $\beta$  decay of  $^{179}\text{Hf}$  followed by neutron capture on the unstable  $^{179}\text{Ta}$ . Beer and Ward [4] suggested a population of  $^{180}\text{Ta}^m$  through a weak  $\beta$ -decay branch of the  $J^\pi = 8^-$  isomer in  $^{180}\text{Hf}$ . However, this mechanism is largely excluded on the basis of a recent measure-

ment of the branching ratio [5]. Substantial production is also predicted in the neutrino  $\nu$  process [6], where inelastic neutrino scattering in a supernova excites giant resonances that subsequently decay by neutron emission. Other mechanisms discussed are interstellar spallation [7] or photodisintegration [8] reactions.

The problem is further aggravated by the possibility of photodeexcitation of the isomer which could drastically alter the half-lives of both states in the  $s$ -process environment [9,10]. This reaction involves resonant excitation into a higher-lying intermediate state (IS) and a finite branching ratio for a subsequent decay cascade to the g.s. as depicted schematically in Fig. 1. Searches for such levels with energies  $E_x < 1.3$  MeV using intense  $^{60}\text{Co}$  and  $^{137}\text{Cs}$  sources were unsuccessful [9,11]. Depopulation of  $^{180}\text{Ta}^m$  was, however, observed after irradiation by several MeV bremsstrahlung [10–12], but the energy of the IS could not be deduced. Recently, the activation function of the  $^{180}\text{Ta}^m(\gamma, \gamma')^{180}\text{Ta}$  reaction using the bremsstrahlung facility at the injector of the S-DALINAC electron accelerator [13] was measured in the energy range 2–7 MeV and intermediate levels could be identified at  $E_x = 2.8$  and 3.6 MeV [14]. Those energies lie too high to be populated in the stellar photon bath at typical  $s$ -process temperatures, but the very large observed integrated cross sections point towards strong  $K$  mixing at fairly low excitation energies. There has been some debate about the magnitudes of the measured cross sections [15,16]. Large isomer photoexcitation cross sections were, however, shown to be a rather general phenomenon in deformed nuclei [17,18]. Furthermore, independent absolute calibration methods of the bremsstrahlung spectra were developed [19] confirming the results of Ref. [14].

\*On leave from Niels Bohr Institute, 2100 Copenhagen, Denmark.

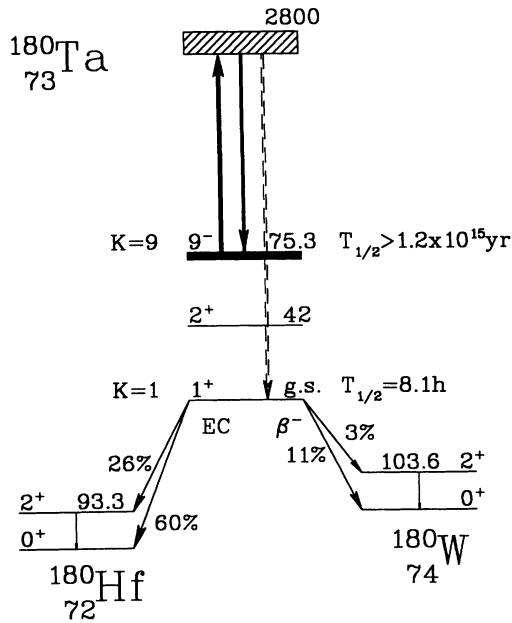


FIG. 1. Relevant  $^{180}\text{Ta}$  levels. Excitation energies are given in keV. The reaction mechanism is schematically indicated for the  $E_x = 2800$  keV level observed in Ref. [14]: Resonant excitation of the  $9^-$  isomer (solid arrow up) followed by a branch into a decay cascade ending up in the  $1^+$  ground state (dashed arrow). The ground-state decay ( $T_{1/2} = 8.1$  h) into  $^{180}\text{Hf}$  and  $^{180}\text{W}$  is also indicated.

The present work describes an investigation of the electromagnetic depopulation of  $^{180}\text{Ta}^m$  with an alternative tool, viz., Coulomb excitation. The purpose of the experiment was twofold: Because of the different selectivity of the Coulomb excitation process involving virtual photons as compared to real photons in the  $(\gamma, \gamma')$  reaction, it was hoped that the multipole character of the upward transition to the IS at  $E_x = 2.8$  MeV could be determined. In addition, it opened the prospect of an alternative search for IS coupling from the isomer to the ground state at astrophysical relevant excitation energies with improved sensitivity limits, at least for  $E2$  or higher multipole transitions.

Several features must be considered. The steep energy dependence of the virtual photon spectrum in Coulomb excitation requires a high- $Z$  projectile in order to achieve measurable population of a level as high as  $E_x = 2.8$  MeV. The experiment has to be of an activation type in order to enable the out-of-beam detection of the signature transitions indicated in Fig. 1 for the decay of the ground state ( $2^+ \rightarrow 0^+$  transition in  $^{180}\text{Hf}$  following electron capture and Hf  $K_\alpha$  x rays).

The importance of neutron pickup reactions on the abundant  $^{181}\text{Ta}$  in the target as an alternative path to populate the ground state of  $^{180}\text{Ta}$  introduces a major uncertainty in the experiment. Although measurements were performed at bombarding energies well below the Coulomb barrier, the yield contributions from these re-

actions may be non-negligible because of the  $10^4$  times higher relative abundance of  $^{181}\text{Ta}$ . Therefore, two different isotopes,  $^{32}\text{S}$  and  $^{36}\text{S}$ , were used as projectiles. They should lead to similar Coulomb excitation yields, but the  $^{32}\text{S}(^{181}\text{Ta}, ^{180}\text{Ta})^{33}\text{S}$  and  $^{36}\text{S}(^{181}\text{Ta}, ^{180}\text{Ta})^{37}\text{S}$  reactions have quite different  $Q$  values (+1.02 MeV and  $-3.27$  MeV, respectively). According to the g.s.-to-g.s.  $Q$ -value systematics in heavy-ion transfer reactions [20] this should lead to cross sections differing at least by an order of magnitude for the two projectiles. A comparison of both measurements should thus allow one to disentangle possible contributions from sub-Coulomb transfer processes to the population of the  $^{180}\text{Ta}$  ground state.

## II. EXPERIMENT AND DATA ANALYSIS

The experiment was performed at the Munich tandem accelerator. Beams of 70–130 MeV  $^{32}\text{S}$  and  $^{36}\text{S}$  ions of typically 400 particle nA were stopped in natural tantalum disks of 0.5 mm thickness and 1 cm diameter. The incident energies were chosen to lie below the critical value of about 130 MeV where nuclear interactions become important [21]. The targets were placed in the bottom of a brass cup of 2.0 cm length and 1.0 cm diameter which provided water cooling on the back side to remove the beam energy deposited in the Ta disks. A ring electrode connected to  $-300$  V was placed at the cup's entrance to repel backward emitted electrons for accurate charge collection. Typical bombarding times were 2 h. The collected charge was continuously monitored and the value stored every 15 s for off-line correction of the  $^{180}\text{Ta}$  g.s. activation due to fluctuations of the beam current.

After irradiation, the Ta disks were placed in front of a well-shielded hpGe detector and the  $\gamma$ -ray spectrum was recorded for typically 2 h. Figure 2 displays a  $\gamma$  spectrum of the radioactivity induced by the bombardment of Ta with  $^{36}\text{S}$  ions at  $E_0 = 130$  MeV. Both types of transitions which can serve as a signature of the  $^{180}\text{Ta}$  g.s. decay were identified: the Hf  $K_{\alpha_1, \alpha_2}$  lines at 54.6 and 55.8 keV and the  $^{180}\text{Hf}$ ,  $2^+ \rightarrow 0^+$  transition at 93.2 keV. The intensities of these lines were used to determine the  $^{180}\text{Ta}$  g.s. population. The observed counts were corrected for the finite duration of irradiation and detection, the absolute efficiency of the detector, and the relative emission probability of the respective signature radiation. A strong background line at  $E_\gamma = 90.6$  keV hampered the analysis of the  $^{180}\text{Hf}$ ,  $2^+ \rightarrow 0^+$  transition and limited it to the higher bombarding energies.

This line and other background lines visible in Fig. 2 can be traced back to fusion reactions with carbon and oxygen impurities leading to a variety of radioactive daughter nuclei. As an example, the strong lines at  $E_\gamma = 62.2$ , 90.6, and 152.9 keV result from the  $^{49}\text{Cr}$  decay which is the  $3n$  decay channel of the  $^{52}\text{Cr}$  compound nucleus resulting from a  $^{36}\text{S} + ^{16}\text{O}$  fusion reaction. Similarly, the  $E_\gamma = 159.3$  keV transition is explained as  $^{47}\text{Sc}$  decay populated in  $^{36}\text{S} + ^{12}\text{C} \rightarrow ^{48}\text{Cr}^*$  reactions. Besides the Hf x rays resulting from the  $^{180}\text{Ta}$  g.s. decay, also Ta x rays are identified. Their excitation stems from the

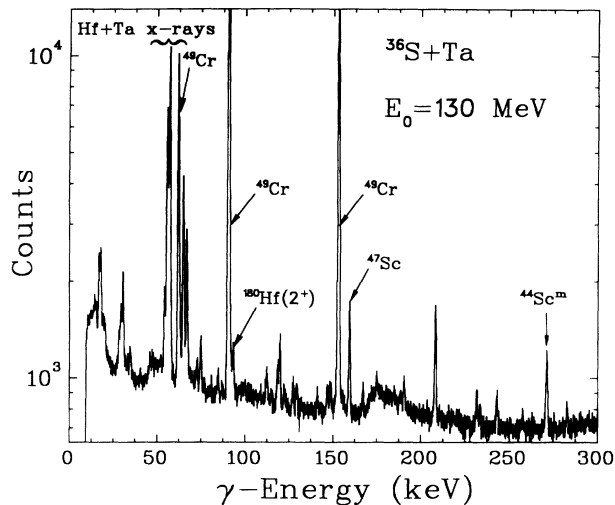


FIG. 2. Spectrum of  $\gamma$  rays following the bombardment of  $^{nat}\text{Ta}$  with 130 MeV  $^{36}\text{S}$  ions. The transitions characteristic for a decay of the  $^{180}\text{Ta}$  g.s. are identified (Hf  $K_{\alpha}$  x rays,  $^{180}\text{Hf}$ ,  $2^+ \rightarrow 0^+$ ). The strong background lines arise from fusion reactions of the projectile with C and O impurities. The respective radioactive daughter isotopes are indicated.

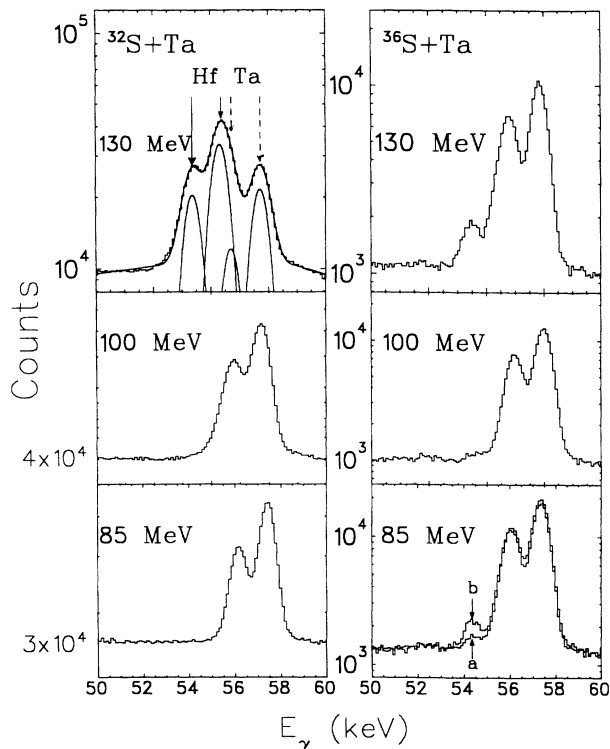


FIG. 3. The expanded 50–60 keV region of the photon decay spectra after irradiation by  $^{32}\text{S}$  and  $^{36}\text{S}$  beams with incident energies  $E_0 = 85, 100,$  and  $130$  MeV. In the upper left part the decomposition of the Hf and Ta  $K_{\alpha}$  x rays is shown. The arrows indicate the energies of the  $K_{\alpha_1}$  and  $K_{\alpha_2}$  lines taken from the literature [22]. The histogram labeled *b* in the lower right part is a decay spectrum recorded after a cooling period of 2 h following the end of the irradiation compared to the normal spectrum labeled *a*. The intensity is normalized to the  $E_{\gamma} = 57.5$  keV peak. One observes an enhancement of the Hf relative to the Ta x-ray count rates.

$\beta$ -radioactivity electrons ionizing the Ta atoms.

Figure 3 shows the expanded 50–60 keV region of the decay spectra for both projectiles and for incident energies  $E_0 = 85, 100,$  and  $130$  MeV as examples. Because of the different compound nuclei produced by the two sulphur isotopes, the overall background in the  $^{32}\text{S}$ -induced spectra is about an order of magnitude larger. In the upper left part the energies of the  $K_{\alpha_1}, K_{\alpha_2}$  x-ray lines are indicated by arrows for Hf and Ta, respectively. The Hf/Ta count-rate ratio becomes smaller and smaller with decreasing incident energy. In order to extract the Hf  $K_{\alpha}$  yields under these conditions a multi-Gaussian fit was performed with the experimentally determined line width and the energy difference of Hf and Ta  $K_{\alpha}$  lines kept fixed. The resulting  $K_{\alpha_1, \alpha_2}$  energies and relative intensity ratios were in good agreement with known values [22] and the total  $K_{\alpha}$  intensities were used in the analysis. An example of the fitting procedure is displayed in the upper left part of Fig. 3.

Because the low Hf/Ta x-ray intensity ratio at the lower bombarding energies was close to the detection limit, an alternative analysis was performed utilizing the fact that the main background radioactive decays, which induce the Ta x rays, have shorter half-lives than the g.s. decay of  $^{180}\text{Ta}$ . The lower right part of Fig. 3 demonstrates for the  $^{36}\text{S}$ ,  $E_0 = 85$  MeV spectrum that the Hf/Ta x-ray ratio can be improved by delaying the start of the detection time with respect to the end of the irradiation (at the price of some loss in statistics). As an example, a gamma spectrum where the measurement started after a cooling time of 2 h is shown labeled *b* while the normal spectrum is labeled *a*. The latter spectrum is normalized to have the same intensity of the  $E_{\gamma} = 57.5$  keV peak. It is evident that the signature transitions at the lowest bombarding energies can be enhanced by letting the background decay away.

### III. RESULTS

Excitation functions for the production of  $^{180}\text{Ta}$  in its g.s. by  $^{32}\text{S}$  and  $^{36}\text{S}$  projectiles are shown in Fig. 4. They are compared to calculations for Coulomb excitation (short-dashed lines) and for single-nucleon transfer (long-dashed lines), respectively. The yield  $Y$  in a thick-target experiment is related to the Coulomb excitation cross section  $\sigma(E)$  by

$$Y = N_T \int_{E_0}^0 \frac{\sigma(E)}{(dE/dx)} dE, \quad (1)$$

with  $dE/dx$  being the energy loss of the projectile and  $N_T$  the density of target atoms. The integral was computed numerically using the values given by Ziegler [23] for  $dE/dx$ .

Transfer cross sections for the reactions  $^{32,36}\text{S}(^{181}\text{Ta}, ^{180}\text{Ta})^{33,37}\text{S}$  were estimated using the coupled-channels code PTOLEMY [24]. Given the odd-odd character of  $^{180}\text{Ta}$ , assignment of quantum numbers to the single-particle orbitals involved in the transition is not unique. The strategy was then to run a series

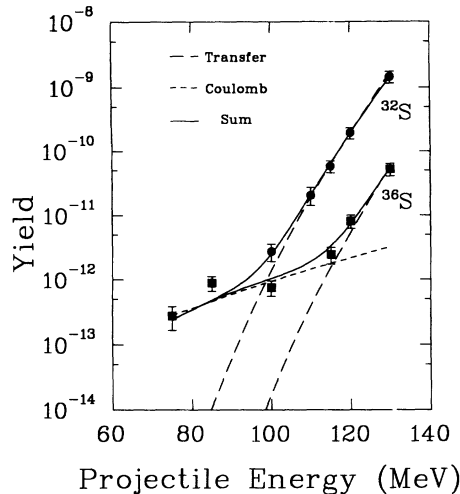


FIG. 4. Yield excitation functions of the  $^{180}\text{Ta}$  g.s. production in bombardments of  $^{\text{nat}}\text{Ta}$  with  $^{32}\text{S}$  and  $^{36}\text{S}$ . The solid circles and squares describe the summed  $K_\alpha$  yields obtained for  $^{32}\text{S}$  and  $^{36}\text{S}$  projectiles, respectively. The long-dashed lines describe the contributions due to the  $^{32,36}\text{S}(^{181}\text{Ta}, ^{180}\text{Ta})^{33,37}\text{S}$  reactions. The short-dashed lines correspond to Coulomb excitation and subsequent decay assuming an intermediate level with  $E_x = 500$  keV and  $B(E2) = 0.08$  W.u. The solid line is the sum of both components.

of calculations for different sets of input parameters (including some for neighboring nuclei) and use the family of results to judge the accuracy of the predictions. As a result, the absolute values of the transfer cross sections can only be considered as order-of-magnitude estimates. The energy dependence and the relative cross sections between the two sulphur isotopes should, on the other hand, be more reliable. These characteristics follow from the slope of one-neutron transfer form factors and  $Q$ -value considerations which are not much affected by the aforementioned ambiguities. The long-dashed curves in Fig. 4 [integrated as in Eq. (1) over energy loss in the target] have been normalized to match the data points at the highest bombarding energies. This adjustment falls well within the range of absolute cross sections predicted by the calculations.

The energy dependence of the different processes observed in Fig. 4 is distinct. The normalized transfer yields show a much steeper increase with projectile energy than the Coulomb-excitation results and give a good description of both excitation functions down to  $E_0 = 110$  MeV. Thus, at these energies the transfer contributions dominate. At lower incident energies an additional component is evident for  $^{36}\text{S}$ -induced data and also for the  $^{32}\text{S}$  data point at  $E_0 = 100$  MeV. The spectra of the  $^{32}\text{S}$  runs for the lower bombarding energies could not be evaluated because of the much larger background (see Sec. II).

In Fig. 5 the yield remaining after subtraction of the transfer part is compared to calculations assuming Coulomb excitation of  $^{180}\text{Ta}$  through a  $B(E2)$  transition

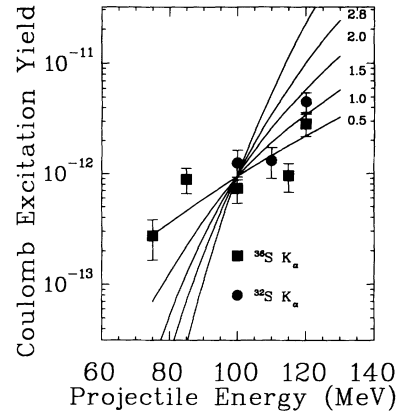


FIG. 5. Comparison of experimental and calculated Coulomb-excitation yields. The solid lines show the excitation-energy dependence of  $E2$  excitation with the curves arbitrarily normalized at  $E_0 = 100$  MeV.

to a single intermediate state and subsequent decay to the g.s. The Coulomb-excitation cross section is a function of the excitation energy and, to first order, proportional to the reduced transition probability.

Calculations are shown for  $E2$  multipolarity and  $E_x = 0.5, 1.0, 1.5, 2.0,$  and  $2.8$  MeV as examples normalized at  $E_0 = 100$  MeV. The excitation-energy dependence is rather strong for higher  $E_x$  and the slope excludes values  $E_x \geq 1$  MeV. For  $E_x \leq 600$  keV the excitation function is almost independent of  $E_x$  and only the reduced transition probability  $B(E2)$  is scaled. Typical ranges are  $B(E2) = 0.02$ – $0.25$  Weisskopf units (W.u.) for  $E_x = 100$ – $1000$  keV, respectively. As an example the short-dashed curve in Fig. 4 shows the Coulomb-excitation cross section for  $E_x = 500$  keV and  $B(E2) = 0.08$  W.u. The solid line, which represents the sum of transfer and Coulomb-excitation contributions, reproduces the experimental yields quite well.

As an alternative to the above interpretation excitation by an  $E3$  transition was considered. The shapes of the calculated excitation functions are almost equal to those of the  $E2$  case, but large reduced transition probabilities are needed to fit the data. The typical range is  $B(E3) = 3$ – $13$  W.u. for  $E_x = 100$ – $1000$  keV. On the other hand, an  $E1$  excitation can be excluded, since it would lead to unrealistically large transition probabilities [ $B(E1) > 1$  W.u.]. For the same reason, higher multiplicities are not taken into account.

We remark that an independent analysis using the data recorded with a 2 h delay with respect to the end of irradiation (see Fig. 3) leads to the same results.

#### IV. DISCUSSION

The large yields due to transfer reactions at the high bombarding energies prevent a conclusion on possible contributions due to Coulomb excitation of the  $E_x = 2.8$  MeV level. Because of the different slopes of the excita-

tion functions for both processes (see Figs. 4 and 5), the Coulomb-excitation contribution to the high bombarding energy yields is limited by the experimental errors to about 10% of the total yield. Assuming a single IS at  $E_x = 2.8$  MeV this would correspond for the  $^{36}\text{S}$ -induced reactions to  $B(E1) \simeq 10$  W.u. and  $B(E2) \simeq 70$  W.u., respectively. Taking into account the estimates deduced from the integrated cross sections of Collins *et al.* [14],  $B(E1) \simeq 0.01$ – $0.05$  W.u.,  $B(M1) \simeq 1$ – $5$  W.u. and  $B(E2) \simeq 60$ – $300$  W.u., an  $E2$  excitation at 2.8 MeV excitation energy can probably be excluded, but nothing can be said about the presence of a contribution due to a dipole excitation; nor can one distinguish between  $E1$  or  $M1$  character. Notwithstanding the large dipole transition strengths indicated by the results of Ref. [14], the corresponding Coulomb-excitation yields of a 2.8 MeV level would represent only a small fraction of the observed yield.

However, the presence of an intermediate level with  $E_x \leq 1$  MeV would have major consequences for the interpretation of possible interstellar production mechanisms. In Fig. 6 the variation of the effective  $^{180}\text{Ta}$  half-life is shown as a function of the stellar photon-bath temperature assuming a mediating level at  $E_x = 500$  keV and 1 MeV, respectively, coupling isomer and g.s. The approach is described in detail in Ref. [10]. The solid lines correspond to a calculation with the transition strength normalized to the experimental Coulomb-excitation yield in Fig. 5. For  $E_x = 500$  keV one observes equilibration at temperatures below  $2 \times 10^8$  K which reduces the value of the g.s. half-life to the laboratory value, corrected for ionization effects in the stellar medium [9,10] assuming an electron density of  $10^3$  g/cm $^3$  for pure He stellar matter. Such a coupling would probably exclude any production in the  $s$  process at commonly adopted [25] temperatures of  $2.8$ – $3.8 \times 10^8$  K. Then  $^{180}\text{Ta}$  might constitute a benchmark for the test of the recently proposed  $\nu$  process [26]

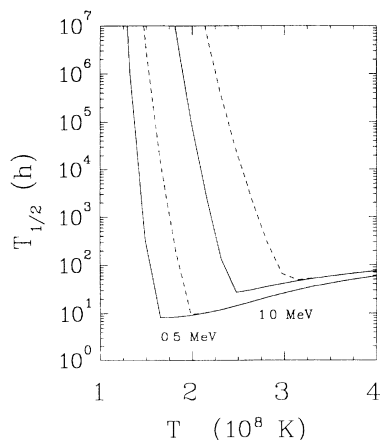


FIG. 6. Effective half-life of  $^{180}\text{Ta}$  as a function of the stellar photon-bath temperature assuming an intermediate state at  $E_x = 500$  keV or 1 MeV coupling the isomer and the g.s. The solid lines correspond to the assumption of a  $B(E2)$  transition to the mediating level and the dashed lines to a  $B(E3)$  transition. The corresponding transition strengths were normalized to the experimental data in Fig. 5.

where significant contributions to the  $^{180}\text{Ta}$  production are claimed [6].

If one allows for higher excitation energies up to  $E_x \approx 1$  MeV, the reduction of the effective isomer half-life depends critically on the multipolarity, the exact energy and partial width of the IS, and the temperature of the stellar photon bath. One obtains parameter regions of extreme temperature dependence similar to what was recently found in  $^{176}\text{Lu}$  where a photon coupling of the  $J^\pi = 7^-$  g.s. and the  $E_x = 123$  keV,  $J^\pi = 1^-$ ,  $T_{1/2} = 3.7$  h isomer through a  $J^\pi = 5^-$  level at 839 keV was identified [27,28]. This is also an initial  $E2$  excitation.

The assumption of an  $E3$  upward transition to the IS shown as dashed lines would lead to a shift of the equilibration temperature to somewhat higher values. However, the main conclusions drawn for the case of an  $E2$  transition still hold since, e.g., for  $E_x = 0.5$  MeV equilibration is reached well below the typical  $s$ -process temperature range.

It is interesting to judge whether the present results are compatible with experimental upper limits deduced from the  $(\gamma, \gamma')$  experiments. Here, only  $E2$  excitation is considered explicitly since the partial widths for gamma excitation become very small with increasing multipolarity. The null results of Ref. [14] at bremsstrahlung end point energies below 2.8 MeV are consistent with  $B(E2) \leq 20$ – $40$  W.u. for  $E_x < 2$  MeV with little excitation energy dependence [29]. An estimate for the measurements using strong  $^{60}\text{Co}$  sources [9,11] is more difficult since the derivation of the partial width  $\Gamma$  from the experimental cross section depends on the unknown photon flux at the resonant energy, i.e.,  $\Gamma \sim \sigma_{\text{expt}}/n_\gamma$ , where  $n_\gamma$  represents the number of resonant photons per energy interval.

For the experimental conditions of Ref. [9] using a medical-therapy  $^{60}\text{Co}$  source the Monte Carlo simulations described in Ref. [30] provide a reasonable estimate of  $n_\gamma \simeq 10^{-6}$ – $10^{-7}$  eV $^{-1}$ . At the highest possible energy of about 1.3 MeV (just below the 1.33 MeV line) the most stringent limit of  $B(E2) \simeq 5$ – $50$  W.u. results. Towards lower energies the limit increases because of the strong  $E_x^5$  dependence of  $\Gamma$ .

In Ref. [11] the Ta cross sections are given as a ratio to the well-established [19,31]  $^{115}\text{In}(\gamma, \gamma')^{115}\text{In}^m$  reaction cross sections. If one assumes that the level at 1.078 MeV in  $^{115}\text{In}$  dominates the isomer cross section for irradiation with a  $^{60}\text{Co}$  source, one can derive from Ref. [11] an upper limit of  $B(E2) \simeq 1$  W.u. for an intermediate state at the same energy. Again, this limit becomes much higher if the excitation energy of the IS is lower.

The above mentioned example of the 839 keV transition in  $^{176}\text{Lu}$  demonstrates that the IS strength derived might be large for a highly  $K$ -forbidden transition, but this is not uncommon. In  $^{176}\text{Lu}$ , where the transition connects the  $K = 7$  g.s. to the  $K = 1$  isomer, the experimental lifetime limits and the measured branching ratio [27] can be converted to  $B(E2) \simeq 0.002$ – $0.5$  W.u. Finally, we mention the possibility to explain the deduced  $B(E3)$  or  $B(E2)$  values through one or more intermediate isomers in the decay cascade providing the large  $\Delta K$  whose

existence cannot be excluded on the basis of the scarce spectroscopic information on the  $^{180}\text{Ta}$  level scheme [32].

## V. CONCLUSIONS

The possible deexcitation of the long-lived  $^{180}\text{Ta}$  isomer via Coulomb excitation was investigated in a thick-target experiment using  $^{32}\text{S}$  and  $^{36}\text{S}$  ions at energies  $E_0 = 70\text{--}130$  MeV. At the higher bombarding energies the  $^{180}\text{Ta}$  g.s. production yield is dominated by the  $^{32,36}\text{S}(^{181}\text{Ta}, ^{180}\text{Ta})^{33,37}\text{S}$  reactions that overshadow any possible observation of the Coulomb excitation of the IS observed in photon scattering at  $E_x = 2.8$  MeV [14]. At lower incident energies the yield excitation functions indicate the presence of an additional contribution attributed to the Coulomb excitation. This component can best be accounted for by assuming a single  $E2$  transition to an intermediate level with  $E_x = 100\text{--}600$  keV and a reduced transition strength of  $B(E2) = 0.02\text{--}0.1$  W.u. This range of values, although large for a highly  $K$ -forbidden transition, is comparable to a similar case in  $^{176}\text{Lu}$ . The upper limits deduced from photon-scattering experiments do not contradict this result. Alternatively, an  $E3$  transition with  $B(E3) = 3\text{--}5.5$  W.u. describes the data equally well.

The identification of an IS at an excitation energy below about 700 keV would have serious consequences for the stellar production mechanism of  $^{180}\text{Ta}$ . The isomer-g.s. system would be equilibrated in the stellar photon bath present during the  $s$  process, thus excluding production of the long-lived isomer in any  $s$ -process scenario. This would make  $^{180}\text{Ta}$  an ideal test case for the recently

proposed  $\nu$  process which claims non-negligible contributions to the  $^{180}\text{Ta}$  nucleosynthesis [6]. If the IS is found at somewhat higher energies, which cannot be excluded because of the fairly large scattering of experimental data, the modification of the isomer effective half-life is hard to predict because of its extreme sensitivity to the temperature of the stellar photon bath.

An independent confirmation of these results would be very desirable, given the experimental difficulties described above. A possible way might be a repetition of the experiment using an intense  $p$  or  $\alpha$  beam where the neutron pickup transfer reaction is suppressed and the background radioactivity from fusion reactions with C and O does not interfere. Alternatively, one can try to identify the IS in in-beam measurements with enriched targets or by using a  $^{180}\text{Ta}$  beam. It is hoped that such experiments presently prepared in Munich and at GSI [33] might allow further insight into the very strong intermediate transitions at  $E_x = 2.8$  and 3.6 MeV observed in Ref. [14] which yet lack explanation.

## ACKNOWLEDGMENTS

We would like to thank J.J. Carroll, C.B. Collins, J. Gerl, F. Riess, and H.J. Wollersheim for stimulating discussions and M. Loewe for assistance during the experiment. C.H.D. gratefully acknowledges a Guest Professorship sponsored by the Heraeus foundation. This work was supported by the Bundesministerium für Forschung und Technologie, Contract No. 06DA641I, and by the Deutsche Forschungsgemeinschaft, Grant No. BO 1109/1.

- 
- [1] J.B. Cummings and D.E. Alburger, *Phys. Rev. C* **31**, 1494 (1985).
- [2] F. Käppeler, H. Beer, and K. Wisshak, *Rep. Prog. Phys.* **52**, 945 (1989).
- [3] K. Yokoi and K. Takahashi, *Nature (London)* **305**, 198 (1983).
- [4] H. Beer and R.A. Ward, *Nature (London)* **291**, 308 (1981).
- [5] S.E. Kellogg and E.B. Norman, *Phys. Rev. C* **46**, 1115 (1992).
- [6] S.E. Woosley, D.H. Hartmann, R.D. Hofmann, and W.C. Haxton, *Astrophys. J.* **356**, 272 (1990).
- [7] K.L. Hainebach, D.N. Schramm, and J.B. Blake, *Astrophys. J.* **205**, 920 (1976).
- [8] T.G. Harrison, *Astrophys. Lett.* **17**, 61 (1976); **18**, 8 (1976).
- [9] E.B. Norman, S.E. Kellogg, T. Bertram, S. Gil, and P. Wong, *Astrophys. J.* **281**, 360 (1984).
- [10] J.J. Carroll, J.A. Anderson, J.W. Glesener, C.D. Eberhard, and C.B. Collins, *Astrophys. J.* **344**, 454 (1989).
- [11] Zs. Németh, F. Käppeler, and G. Reffo, *Astrophys. J.* **392**, 277 (1992).
- [12] C.B. Collins, C.D. Eberhard, J.W. Glesener, and J.A. Anderson, *Phys. Rev. C* **37**, 2267 (1988).
- [13] K. Alrutz-Ziemssen, D. Flasche, H.D. Gräf, V. Huck, M. Knirsch, W. Lotz, A. Richter, T. Rietdorf, P. Schardt, E. Spamer, A. Stascheck, W. Voigt, H. Weise, and W. Ziegler, *Part. Accel.* **29**, 53 (1990).
- [14] C.B. Collins, J.J. Carroll, T.W. Sinor, M.J. Byrd, D.G. Richmond, K.N. Taylor, M. Huber, N. Huxel, P. von Neumann-Cosel, A. Richter, C. Spieler, and W. Ziegler, *Phys. Rev. C* **42**, R1813 (1990).
- [15] Zs. Németh, *Phys. Rev. C* **45**, 467 (1992).
- [16] J.J. Carroll, C.B. Collins, P. von Neumann-Cosel, D.G. Richmond, A. Richter, T.W. Sinor, and K.N. Taylor, *Phys. Rev. C* **45**, 472 (1992).
- [17] C.B. Collins, J.J. Carroll, K.N. Taylor, D.G. Richmond, T.W. Sinor, M. Huber, P. von Neumann-Cosel, A. Richter, and W. Ziegler, *Phys. Rev. C* **46**, 952 (1992).
- [18] J.J. Carroll, C.B. Collins, K. Heyde, M. Huber, P. von Neumann-Cosel, V.Yu. Ponomarev, D.G. Richmond, A. Richter, C. Schlegel, T.W. Sinor, and K.N. Taylor, *Phys. Rev. C* **48**, 2238 (1993).
- [19] P. von Neumann-Cosel, N. Huxel, A. Richter, C. Spieler, J.J. Carroll, and C.B. Collins, *Nucl. Instrum. Methods A* **338**, 425 (1994).
- [20] A.G. Artukh, V.V. Ardeichikov, J. Erö, G.F. Gridnev, V.L. Mikheev, V.V. Volkov, and J. Wylczynsky, *Nucl. Phys. A* **160**, 511 (1971).
- [21] K. Alder and A. Winther, *Electromagnetic Excitations: Theory of Coulomb Excitation with Heavy Ions* (North-Holland, Amsterdam, 1975).

- [22] *Table of Isotopes*, 7th ed., edited by C.M. Lederer and V.S. Shirley (Wiley, New York, 1978).
- [23] J.F. Ziegler, *Stopping Cross Sections for Energetic Ions in all Elements* (Pergamon, New York, 1980), p. 364.
- [24] D.H. Gloeckner, M.H. Macfarlane and S.C. Pieper, computer program PTOLEMY, Argonne National Laboratory Report No. ANL-76-11, 1978 (unpublished); M. Rhoades-Brown, M.H. Macfarlane, and S.C. Pieper, Phys. Rev. C **21**, 2417 (1980); **21**, 2436 (1980).
- [25] F. Käppeler, R. Gallino, M. Busso, G. Picchio, and C.M. Raiteri, *Astrophys. J.* **354**, 630 (1990).
- [26] W.C. Haxton, Phys. Rev. Lett. **60**, 1999 (1988).
- [27] N. Klay, F. Käppeler, H. Beer, and G. Schatz, Phys. Rev. C **44**, 2839 (1991).
- [28] K.T. Lesko, E.B. Norman, R.-M. Larimer, B. Sur, and C.B. Beausang, Phys. Rev. C **44**, 2850 (1991).
- [29] J.J. Carroll (private communication).
- [30] P. von Neumann-Cosel, A. Richter, J.J. Carroll, and C.B. Collins, Phys. Rev. C **44**, 554 (1991).
- [31] P. von Neumann-Cosel, A. Richter, C. Spieler, W. Ziegler, J.J. Carroll, T.W. Sinor, D.G. Richmond, K.N. Taylor, C.B. Collins, and K. Heyde, Phys. Lett. B **266**, 9 (1991).
- [32] E. Browne, Nucl. Data Sheets **71**, 81 (1994).
- [33] J. de Boer, A. Lössch, M. Loewe, H.J. Maier, C.H. Dasso, E. Hechtel, P. von Neumann-Cosel, A. Richter, and C. Schlegel, contribution to EPS9: Trends in Physics, Florence, Italy, 1993 (unpublished).